QCM Immunoassay for Phosphorylated Acetylcholinesterase as a Biomarker for Organophosphate Exposures Based on Selective Zirconia Adsorption and Enzyme-Catalytic Precipitation

Hua Wang[†], **Jun Wang**, **Daiwon Choi**, **Zhiwen Tang**, **Hong Wu**, and **Yuehe Lin**[*]
Pacific Norwest National Laboratory, Richland, WA, 99352

Abstract

A zirconia (ZrO_2) adsorption-based immunoassay by electrochemical quartz crystal microbalance (EQCM) has been initially developed, aiming at the detection of phosphorylated acetylcholinesterase (Phospho-AChE) as a potential biomarker for bio-monitoring exposures to organophosphate (OP) pesticides and chemical warfare agents. Hydroxyl-derivatized monolayer was preferably chosen to modify the crystal serving as the template for directing the electro-deposition of ZrO_2 film with uniform nanostructures. The resulting ZrO_2 film was utilized to selectively capture Phospho-AChE from the sample media. Horseradish peroxidase (HRP)-labeled anti-AChE antibodies were further employed to recognize the captured phosphorylated proteins. Enzyme-catalytic oxidation of the benzidine substrate resulted in the accumulation of insoluble product on the functionalized crystal. Ultrasensitive EQCM quantification by mass-amplified frequency responses as well as rapid qualification by visual color changes of product could be thus achieved. Moreover, 4-chloro-1-naphthol (CN) was studied as an ideal chromogenic substrate for the enzyme-catalytic precipitation. Experimental results show that the developed EQCM technique can allow for the detection of Phospho-AChE in human plasma with a detection limit of 0.020 nM. Such an EQCM immunosensing format opens a new door towards the development of simple, sensitive, and field-applicable biosensor for biologically monitoring low-level OP exposures.

Keywords

Phosphorylated acetylcholinesterase; Zirconia; Enzyme-catalytic precipitation; EQCM; Organophosphate exposures

1. Introduction

Organophosphates (OPs), which are commonly used as pesticides and chemical warfare agents, are highly neurotoxic. How to detect these toxic agents in the environment and public places or workplaces especially to evaluate the human health risk of OP exposures has been a very active research area.(Noort et al. 2002; Noort et al. 2006; Worek et al. 2005) After the tragic "9.11" event, public concerns about the development of rapid and effective analysis techniques

*Corresponding author, e-mail: yuehe.lin@pnl.gov; Tel: 01-509-376-0529.
[†]Permanent Address: State Key Laboratory for Chemo/Biosensing and Chemometrics, College of Chemistry and Chemical Engineering, Hunan University, Changsha 410082, China.

for OP monitoring have been increasing steadily.(Noort et al. 2002; Noort et al. 2006; Worek et al. 2005) At present, the detection of OPs in environmental and biological samples is routinely carried out using analytical techniques, such as gas or liquid chromatography and mass spectrometry.(Fidder et al. 2002; Noort et al. 2006; Polhuijs et al. 1997; Read and Black 1999) The methods, however, generally require extensive labor, lengthy turnaround time, and large-sized analysis settings, which may prohibit them from being used for rapid analysis under field conditions. Recently, portable OP pesticide kits have become commercially available, but present qualitative or semi-quantitative results in addition to complicated handling procedures.(Liu and Lin 2005) Alternatively, considerable efforts have been contributed to the development of a diverse range of biosensors for OP detections in both environmental and biological systems.(Liu and Lin 2005; Mulchandani et al. 1999; Pavlov et al. 2005; Sacks et al. 2000; Schulze et al. 2004; Simonian et al. 2005) These portable devices are thought to well meet the requirements of decentralized point–of-care tests or field detections with portable instrument and simple operation.(Cousino et al. 1997; Pumera et al. 2007; Zhang 2007)

It is recognized that once entering the human or animal body, OPs can covalently bind with cholinesterase (ChE) to conduct the enzyme inhibition effects, at the meantime, they may be decomposed by organophosphorus hydrolase to form inactive phosphonic acids that are renally excreted.(He 1999) Accordingly, common biomarkers for probing internal OP dosimetry mainly include free OPs in blood, or their metabolites in urine, and ChE inhibition-based biological effects.(He 1999;He et al. 2002;Noort et al. 2002;Wessels et al. 2003) However, the high reactivity of OPs with the enzymes suggests that the blood levels of free OPs will be inherently low (typically seen in the range of nanogram per liter or parts per trillion in blood (Wessels et al. 2003). Ultra-sensitive methodologies for detecting free OPs in body are thereby required. Moreover, OP metabolite level in urine is also considered a sensitive indicator of OP exposures,(He 1999;Liu et al. 2005) however, it may be challenged by the urine output varies and the fact that not all toxicant specific metabolites are derived solely from OPs. Also, the enzyme inhibition-based OP quantification may have even more disadvantages. (Simonian et al. 2005;Wessels et al. 2003) For example, a baseline enzyme level is also required to be determined prior to the sample tests due to the fluctuations in enzyme levels for diverse individuals. Therefore, exploring a more effective and sensitive biomarker for evaluation of OP exposures is of considerable interest.

According to the biochemical mechanism established for the phosphorylation of ChE (i.e., AChE), (Kwong 2002; Mileson et al. 1998) the inhibition event may produce very stable enzyme complexes with structurally precise phosphoserine esters.(George et al. 2003) The so produced phosphorylated ChE is assumed to be a new biomarker correlating to the severity of original OP exposures. However, the detection of such a new biomarker can be challenged by the unavailability of specific recognition elements or receptors, i.e., antibodies. Recent researches have demonstrated that some transitional metal oxides such as zirconia (ZrO_2) can have a strong affinity for phosphoric groups and are used as capturing agents for selectively enriching free OP and phosphorylated peptides.(Kweon and Hakansson 2006; Liu and Lin 2005) In this current work, we try to introduce synergistically ZrO_2 nanoparticles and horseradish peroxidase (HRP) labeled anti-AChE antibodies (HRP-anti-AChE) as selective sorbents and immunorecognition receptors to detect phosphorylated AChE (Phospho-AChE) as a potential biomarker for bio-monitoring OP exposures. Electrochemical quartz crystal microbalance (EQCM) was employed as the real-time transducer. Phospho-AChE is selectively captured by ZrO_2 nanoparticles electro- deposited on the crystals, and then recognized by HRP-anti-AChE. The so bound HRP will catalyze the H_2O_2-induced oxidation of 4-chloro-1-naphthol (CN) substrate to form an insoluble precipitation on the crystals, thus causing frequency changes (Δf) that are proportional to the concentrations of targeting Phospho-AChE. The main advantage of this enzyme-catalytic precipitation protocol lies in that the accumulation of an insoluble product on the crystals can lead to greatly increased mass

changes as reflected by Δf (Alfonta et al. 2000; Ebersole and Ward 1988; Patolsky et al. 1999; Su and Li 2001). It can achieve much higher detection sensitivity than some traditional EQCM methods with mass changes directly originating from the adsorption of the analytes or even the enzyme-labeled antibodies. To our best knowledge, this is the first report regarding the development of ZrO_2 adsorption-based EQCM immunosensor for the determination of Phospho-AChE for bio-monitoring the exposures to OP pesticides and chemical warfare agents.

2. Experimental

2.1. Reagents

Human acetylcholinesterase (AChE), bovine serum albumin (BSA), CN, paraoxon, zirconium oxychloride ($ZrOCl_2$), 2-mercaptoethanol (ME), N-hydroxysuccinimide (NHS), 1- ethyl-3-[3-dimethylaminopropyl]carbodiimide hydrochloride (EDC), polyethylene glycol (PEG, MW 10 KD), 2-(N-morpholino)ethanesulfonic acid (MES) buffer, hydroxylamine, 3,3′5,5′-tetramethylbenzidine dihydrochloride (TMB), $Tris$-HCl stock buffer (1.0 M), Tween-20, and hydrogen peroxide were purchased from Sigma-Aldrich. Polyclonal anti-AChE antibodies were purchased from Abcam. Human plasma was purchased from Golden West Biologicals, Inc.. The washing buffer was prepared with 0.02 M phosphate buffer saline (PBS, pH 7.2) containing 0.5 % BSA, 0.25 % Tween-20 and 0.15 M NaCl. The BSA-PEG blocking buffer consisted of 3.0 % BSA and 1.0 % PEG. The CN-H_2O_2 substrate mixture was prepared by freshly mixing CN solution in ethanol and H_2O_2, with final concentrations of 1.0 mM and 5.0 mM, respectively. Other reagents were of analytical reagent grade.

2.2. Apparatus

CHI 400 A electrochemical analyzer, crystals (9 MHz, gold electrodes), and EQCM cell system were bought from CH Instruments (Austin, TX), in which the EQCM cell consists of a detection cell and Ag/AgCl reference electrode and Pt wire counter electrode. SEM (JEOL JSM-5900 LV) was used for observing the microstructure of the crystal surface with different modifications. Disposable PD-10 desalting columns packed with Sephadex G-25 medium (Amersham Bioscience Corp.) were utilized to purify the protein solution. Centrifugation was performed using a Sorvall RC 26 plus (Kendro Laboratory Product). Vortex mixer with touch-on-off function of mixing (Barnstead International, Iowa) was used for sample and reactant mixture.

2.3. Electro-deposition of ZrO_2 nanoparticle film

The electro-deposition of ZrO_2 film onto the gold electrode of the crystals was conducted in the EQCM cell system. The crystal was first cyclic-potential scanned within the potential range 0.5 – 1.5 V in freshly prepared 0.2 M H_2SO_4 until a voltammogram characteristics of the clean polycrystalline gold was established. Then, it was washed with distilled water and dried by nitrogen. Following that, 50 μl ME (20 mM) was dropped on the gold electrode to be assembled overnight at 4 °C. ZrO_2 nanoparticles were deposited onto the mercaptoethanol-derivatized in an aqueous electrolyte of 5.0 mM $ZrOCl_2$ and 0.1 M KCl by cycling the potential between −1.1 and + 0.7 V (versus Ag/AgCl) at a scan rate of 20 mV s^{-1} for 5 consecutive scans. The gold electrodes modified with ZrO_2 nanoparticles were rinsed with DI-water and dried in N_2 for further experiments. For purpose of comparison, ZrO_2 film was also deposited on bare gold electrode of the crystal in the same way above. SEM images were recorded to characterize comparably the surface topologies of the ZrO_2 films so formed.

2.4. Preparation of Phospho-AChE

Human AChE (1.1 μM) was mixed with 7.5 mM paraoxon to be incubated overnight at 37 °C. The enzyme activity was measured with the modified Ellman colorimetric method, (Ellman et al. 1961) showing the complete inhibition of AChE activity. Furthermore, the mixture was dialyzed against 0.02 M PBS buffer (pH 7.2) overnight at 4 °C in order to remove the possibly excessive paraoxon. Moreover, the resultant adducts were concentrated by using ultra-filtration to a final volume of ~ 0.40 ml, and stored at − 20 °C for future usage. The protein concentration of the Phospho-AChE solution was determined to be ~ 3.0 μM by spectrophotometry at 280 nm.

2.5. Preparation of HRP-anti-AChE conjugate

HRP was first activated by adding 0.5 mg HRP in 1.0 ml of activation buffer containing 0.10 M MES and 0.50 M NaCl. A total of 0.4 mg of EDC (final concentration ~ 2.0 mM) and 0.6 mg of NHS (final concentration ~ 5 mM) were added to the activated HRP solution to be reacted for 15 min at room temperature. The EDC was quenched by adding 1.4 μl of ME (final concentration of 20 mM). The excess reducing agent and inactivated cross-linker were removed with a PD-10 column. The eluent was collected and concentrated to 1.0 ml in an ultracentrifuge tube. Anti-AChE antibody was added at an equal molar equivalent to HRP in the above solution, and the reaction proceeded for 2 h at room temperature. The reaction was quenched by adding hydroxylamine at a final concentration of 10 mM. Excess hydroxylamine was removed using a PD-10 column. The eluent of HRP-anti-AChE was collected and kept in PBS buffer containing 0.5 % BSA at 4 °C for further use.

2.6. ZrO$_2$ adsorption-based EQCM immunoassays

EQCM immunoassays were performed in the EQCM cell system in which the EQCM analyzer was connected to a laptop computer. An aliquot of 50 μl of Phospho-AChE, which was diluted to the desired concentration with acetate buffer solution (pH 4.0) containing 0.5 % BSA or with human plasma, was injected onto the above ZrO$_2$-coated crystal and incubated for 1.5 h at 37 °C in a humidified chamber. Phospho-AChE attached crystal was then washed three times with the washing buffer. The resulting sensor was blocked for 30 min with the blocking buffer. After washing twice, 50 μl of HRP-anti-AChE (2.5 μg ml^{-1}) was dropped onto the crystal and incubated for 1 h at 37 °C, then, rinsed with the washing buffer. Following that, 50 μl of the CN-H$_2$O$_2$ mixture was added onto the crystal resulting in the enzyme-catalytic precipitation of the CN substrate. The induced frequency changes (Δf) were recorded as the reaction proceeded from 30 s (after the addition of samples) until equilibrium was reached (~ 15 min). The control tests with AChE were performed accordingly. The frequency changes in all experiments were referred to the average responses with corresponding standard deviations ($\pm$ SD) of triplicate measurements, unless otherwise indicated.

In addition, the investigation of pH dependent adsorption of Phospho-AChE on ZrO$_2$ film was carried out by detecting 0.1 nM Phospho-AChE at different pH values with acetate or PBS buffer solutions.

3. Results and Discussion

3.1 Main principle and characteristics of ZrO$_2$ adsorption-based EQCM immunoassays

It is established that upon entering human body, OPs will bind with ChE (i.e., AChE) to conduct the irreversible enzyme inhibition yielding a stable phosphorylated ChE adduct.(George et al. 2003; Kwong 2002; Mileson et al. 1998) This phosphorylated adduct is thought to be a new biomarker which amount in body can correlate to the degree of OP exposures. Moreover, ZrO$_2$ nanoparticles have been demonstrated with strong affinity to phosphoric groups for

selectively binding OPs or phosphorylated peptides.(Kweon and Hakansson 2006; Liu and Lin 2005) In this work, we seek to utilize ZrO_2 nanoparticles and HRP-anti-AChE as selective sorbents and recognition receptors, respectively, to achieve the specific detection of the Phospho-AChE using real-time EQCM. Fig. 1 illustrates the schematic principle for ZrO_2 adsorption-based EQCM immunoassays for Phospho-AChE. The gold electrode of the crystal was first modified with ME monolayer and then electro-deposited with ZrO_2 film. Phospho-AChE adducts were then captured onto the ZrO_2-coated crystal to be further recognized by HRP-anti-AChE. The $CN-H_2O_2$ substrate was subsequently introduced onto the crystal, where enzyme could catalyze a H_2O_2-induced oxidation of CN to form an insoluble product. The time-dependent accumulation of the precipitation on the crystal will cause Δf proportional to the Phospho-AChE concentrations. Herein, the relationship between Δf and mass changes on the crystal can be described by the *Sauerbrey* equation.(Buttry and Ward 1992) Moreover, a red-purple color change can be observed synchronously, thereby facilitating a rapid qualitative assessment of Phospho-AChE as an indictor of OP exposures.

The morphological features of ZrO_2 films formed on the ME-modified and bare gold electrodes were comparably investigated, including their corresponding H_2O_2-oxidized products formed in the subsequent immunoassays (Fig. 2). As can be seen from Fig. 2, the "coral-like islands" of ZrO_2 film on the ME-modified electrode (Fig. 2A) are decorated with more uniform and smaller spherical ZrO_2 particles in nanometer size, comparing with those on the bare gold electrode (Fig. 2C). Moreover, the insoluble precipitations accumulated on the ME-functionalized surface show nanometer-sized particles closely packed (Fig. 2B), in contrast to those on the bare gold surface (Fig. 2D). That is, a larger amount of enzyme-catalytic precipitation products can be obtained for the ME-functionalized surface, resulting from its better electro-deposition features of ZrO_2 film.

Figure 3 manifests the EQCM cyclic voltammograms (CVs) characterizing the step-by-step buildup process of the crystal using $[Fe(CN)_6]^{4-/3-}$ as the probe couple. As can be seen from Fig. 3, a couple of quasi-reversible redox peaks of the probe were obtained at the bare gold electrode of the crystal (Fig. 3a), and a decrease in current response was envisaged upon the assembly of ME monolayer (Fig. 3b). The interfacial electron-transfer resistance of the electrode increased greatly when semi-conductive ZrO_2 film was deposited (Fig. 3c). Moreover, the step-by-step insulation of the conductive surface grew with the protein or polymer modifications of Phospho-AChE (Fig. 2d), BSA-PEG (Fig. 3e), and HRP-anti-AChE (Fig. 3f). The electrical communication between the $[Fe(CN)_6]^{4-/3-}$ probe and the electrode surface was almost inhibited completely after the H_2O_2-oxidized precipitation of CN by enzyme catalysis (Fig. 3g), showing a entirely depleted electrical response. Therefore, the electron-transfer kinetics indicates that ZrO_2 adsorption-based EQCM immunoassays for Phospho-AChE could be achievable following the stepwise performances in the protocol established above.

3.2 Electro-deposition of ZrO_2 nanoparticles templated by hydroxyl-derivatized monolayer

The fabrication of ZrO_2 film with desired micro- to nano-structures is considered of great importance for better adsorption of phosphorylated proteins or peptides. Accordingly, the selection and preparation of micro-patterned substrates, i.e., by creating chemical templates, for inorganic material micro-fabrication are critical issues for consideration.(Azzaroni et al. 2001; Ji et al. 2002; Yu et al. 2002) In the current experiments, the gold electrode of the crystal was modified with ME monolayer serving as the template for the selective growth of ZrO_2 film by electro-deposition. The ZrO_2 film deposited onto bare gold electrode was also conducted for purpose of comparison. The deposition processes were monitored in real time using EQCM, simultaneously showing CVs and Δf (Fig. 4). The formation of the semi-conductive ZrO_2 film on the electrodes could increase the interfacial electron-transfer

resistance, in addition to a mass increase on the transducer as reflected by a decrease in resonance frequency. As can be observed from Fig. 4A, during the electro-deposition process the ZrO_2 polymerization proceeded with gradually decreasing current as repetitive scanning. These CV changes can correspond to the Δf shown in Fig. 4B. Herein, resonance frequencies of the ME-modified electrode decreased reasonably with the layer-by-layer electro-deposition ($\sim 3510 \pm 75$ Hz for five scanning circles), implying that a mass increase on the crystal occurred together with a uniform formation of ZrO_2 film. That is in contrast to the ZrO_2 film electro-deposited onto the bare gold electrode (Fig. 4C). As shown in Fig. 4C, the Δf could decrease as ZrO_2 film was deposited during the initial three scanning cycles, after which the Δf increased suddenly, presumably due to the part desorption of the ZrO_2 film so deposited. Accordingly, ZrO_2 film might be frequently unstable when deposited on the bare gold electrode (6.0 mm in diameter), although the general CV features are quite similar to those of the ME-modified ones (data not shown). More importantly, as aforementioned ZrO_2 films formed on the ME-modified and bare electrodes showed quite different morphological characteristics of SEM images (Fig. 2). Such a phenomenon can be understood by the facts below. On the one hand, $ZrOCl_2$ precursors can be attached to the hydroxyl-terminated monolayer via a ligand exchange reaction of the terminal alcohols of ME with chloride ligands of the precursors.(Yu et al. 2002) On the other hand, when the electrode is modified with the closely packed ME monolayer, the decreased interfacial electron transfer rate can thus allow for a slower and more organized deposition of ZrO_2 nanoparticles with high stability. In addition to being the selective sorbents, the so prepared ZrO_2 film can offer a larger surface area for highly loading enzyme-catalytic precipitation product yielded in the immunoassay step.

3.3. Selective adsorption of ZrO_2 nanoparticles for Phospho-AChE

It is recognized that ZrO_2 possesses amphoteric properties of either as a *Lewis* acid or base depending on the pH of the reaction solution, due to their unsatisfied valencies of both oxygen and zirconium atoms in the surface layer.(Kweon and Hakansson 2006; Nawrocki et al. 1993) Accordingly, high binding selectivity of phosphorylated proteins or peptides over non-phosphorylated ones should be achievable with ZrO_2 upon a careful pH selection. In this current work, the adsorption abilities of ZrO_2 to Phospho-AChE were studied under different pH conditions. Figure 5 manifests the experimental results. Obviously, ZrO_2 film could exhibit better adsorption to Phospho-AChE under the slightly acidic environments, as reflected by relatively high Δf. Herein, ZrO_2 can behave as a *Lewis* acid with positively charged zirconium atoms, (Kweon and Hakansson 2006) thereby providing high binding affinity for phosphoric residues of Phospho-AChE. The formation of chemical bonds between ZrO_2 and phosphorous residues of Phospho-AChE may presumably occur, as schematically illustrated in Fig. 1. Note that too low pH values (i.e., pH $\leq$ 2.0) may cause the denaturation of proteins. The highest adsorption of phosphorylated proteins was achieved at pH 4.0, which is recommended in the current experiments.

Furthermore, the adsorption selectivity of ZrO_2 film to Phospho-AChE adducts was investigated by real-time EQCM monitoring, with AChE as a control (the bottom insert in Fig. 6). It can be discovered that the ZrO_2 adsorptions to 0.5 nM AChE and Phospho-AChE could result in Δf of $\sim 102 \pm 13$ Hz and $\sim 220 \pm 18$ Hz, respectively. Obviously, non-specific adsorption of AChE on ZrO_2 film may be a challenge to some degree. Accordingly, after the adsorptions of Phospho-AChE and AChE, the crystals were washed separately three times by the washing buffer. The Δf could be recovered to $\sim 23 \pm 7$ Hz and $\sim 91 \pm 5$ Hz, respectively. The data indicate that the harsh washing steps could allow the attached AChE to be largely removed, while most Phospho-AChE could be retained. That is, ZrO_2 film can present favorably high adsorption selectivity to Phospho-AChE, if aided by the additional washing steps. Moreover, as can be seen from the bottom insert of Fig. 6, the time for the complete adsorption of Phospho-AChE on ZrO_2 film is about 1.5 h.

3.4. Analysis performances of EQCM immunoassay

It is established that HRP can catalyze the H_2O_2-induced oxidization of some chromogenic substrates, typically as CN and TMB, to form insoluble precipitates towards amplified EQCM assays.(Alfonta et al. 2000; Ebersole and Ward 1988; Patolsky et al. 1999; Su and Li 2001) Nevertheless, our experimental results show that CN is better than TMB as the substrate for enzyme-catalytic precipitation in the EQCM assays (Supporting Information).

Under the optimal experimental conditions, EQCM immunoassays for Phospho-AChE, AChE and BSA were conducted comparably (the top insert in Fig. 6). Obviously, big differences in Δf responses for the final enzyme-catalytic precipitation of CN-H_2O_2 substrate were obtained, indicating the high detection specificity for Phospho-AChE. Moreover, several Phospho-AChE samples with different concentrations in plasma were determined by the developed EQCM immunoassay. Figure 6 describes the calibration curve between Δf versus [Phospho-AChE] plotted on a semi-log scale. As is shown in Fig. 6, a linear response is obtained over the Phospho-AChE concentrations ranging from 0.025 to 10 nM, with a detection limit of 0.020 nM, as estimated by the "S/N = 3" rule. In addition, a change in red-purple color could also be apparently accompanied when the CN-H_2O_2 mixture was added onto the resulting crystal surface for ∼ 10 to 15 min. Rapid qualitative assessments can thus be expected allowing for the visual screening of samples as a result of OP exposures.

After each immunoassay, the used crystals were washed by using 8.0 M urea for 15 ∼ 20 min. It was observed that such a urea regeneration step could cause a gradual increase in frequency responses (data not shown). The adsorbed substances from Phospho-AChE to the final enzyme-catalytic products could be thus peeled off the ZrO_2-modified crystals. In addition, five repetitive measurements for 0.5 nM Phospho-AChE were carried out for the ZrO_2-modified crystal so regenerated, yielding reproducible frequency responses with an RSD of 17.6 %. The above data indicate that the developed EQCM immunoassay can show high sensitivity and reproducibility for detection of Phospho-AChE. Note that human plasma contains about 8.0 ng ml^{-1} (≈ 0.12 nM) AChE. (Brimijoin and Hammond 1988) Accordingly, the developed immunosensing strategy can be tailored as a new method for bio-monitoring the low OP exposures. (Wang et al. 2008)

4. Conclusions

In this work, an EQCM immunoassay using ZrO_2 nanoparticles as selective sorbents has been successfully developed for the first time for detection of Phospho-AChE as a new biomarker for bio-monitoring OP exposures. The synergistic applications of ZrO_2 nanoparticles and HRP labeled anti-AChE antibodies have been verified to well circumvent the specific recognition of targeting Phospho-AChE. H_2O_2 oxidization of the benzidine substrate by HRP catalysis could produce an insoluble precipitation on the crystal resulting in greatly amplified EQCM responses. Herein, the electro-deposition of ZrO_2 film onto the hydroxyl-derivatized crystal could achieve uniform nanostructures with better adsorptions for Phospho-AChE, as compared with those on bare gold electrode. The so deposited ZrO_2 nanoparticle film can provide a larger surface area for loading the enzyme-catalytic product in addition to serving as the selective sorbents. Moreover, CN was verified as the ideal chromogenic substrate suitable for enzyme-catalytic precipitation. Ultrasensitive quantitative and rapid qualitative EQCM analysis of the targets could be expected through mass-amplified frequency responses and visual color changes, respectively. This proposed EQCM immunosensing technique is simple, real-time, sensitive, and field-applicable, holding great promise of being applied as an alternative tool for onsite bio-monitoring the exposures to nerve agents and pesticides.

Supplementary Material

Refer to Web version on PubMed Central for supplementary material.

Acknowledgments

References

Alfonta L, Katz E, Willner I. Anal Chem 2000;72(5):927–935. [PubMed: 10739194]

Azzaroni O, Schilardi PL, Salvarezza RC. Nano Letters 2001;1(6):291–294.

Buttry DA, Ward MD. Chem Rev 1992;92(6):1355–1379.

Brimijoin S, Hammond P. J Neurochem 1988;51:1227–1231. [PubMed: 2901462]

Cousino MA, Jarbawi TB, Halsall HB, Heineman WR. Anal Chem 1997;69(17):A544–A549.

Ebersole RC, Ward MD. J Am Chem Soc 1988;110(26):8623–8628.

Ellman GL, Courtney KD, Andres V, Featherstone RM. Biochem Pharmacol 1961;7(2):88–95. [PubMed: 13726518]

Fidder A, Hulst AG, Noort D, de Ruiter R, van der Schans MJ, Benschop HP, Langenberg JP. Chem Res Toxicol 2002;15(4):582–590. [PubMed: 11952345]

George KM, Schule T, Sandoval LE, Jennings LL, Taylor P, Thompson CM. J Biol Chem 2003;278(46): 45512–45518. [PubMed: 12933813]

He FS. Toxicol Lett 1999;108(2–3):277–283. [PubMed: 10511272]

He FS, Chen SY, Tang XY, Gan WQ, Tao BG, Wen BY. Toxicol Lett 2002;134(1–3):119–124. [PubMed: 12191869]

Ji JM, Li X, Canham LT, Coffer JL. Adv Mater 2002;14(1):41–43.

Kweon HK, Hakansson K. Anal Chem 2006;78(6):1743–1749. [PubMed: 16536406]

Kwong TC. Ther Drug Monit 2002;24(1):144–149. [PubMed: 11805735]

Liu GD, Lin YH. Anal Chem 2005;77(18):5894–5901. [PubMed: 16159119]

Liu GD, Riechers SL, Timchalk C, Lin YH. Electrochem Commun 2005;7(12):1463–1470.

Mileson BE, Chambers JE, Chen WL, Dettbarn W, Ehrich M, Eldefrawi AT, Gaylor DW, Hamernik K, Hodgson E, Karczmar AG, Padilla S, Pope CN, Richardson RJ, Saunders DR, Sheets LP, Sultatos LG, Wallace KB. Toxicol Sci 1998;41(1):8–20. [PubMed: 9520337]

Mulchandani A, Mulchandani P, Chen W, Wang J, Chen L. Anal Chem 1999;71(11):2246–2249.

Nawrocki J, Rigney MP, McCormick A, Carr PW. J Chromatogr A 1993;657(2):229–282. [PubMed: 8130879]

Nineham AW. Chem Rev 1955;55(2):355–483.

Noort D, Benschop HP, Black RM. Toxicol Appl Pharm 2002;184(2):116–126.

Noort D, Fidder A, van der Schans MJ, Hulst AG. Anal Chem 2006;78(18):6640–6644. [PubMed: 16970345]

Patolsky F, Zayats M, Katz E, Willner I. Anal Chem 1999;71(15):3171–3180. [PubMed: 10450161]

Pavlov V, Xiao Y, Willner I. Nano Lett 2005;5(4):649–653. [PubMed: 15826103]

Polhuijs M, Langenberg JP, Benschop HP. Toxicol Appl Pharm 1997;146(1):156–161.

Pumera M, Sanchez S, Ichinose I, Tang J. Sens Actuators B 2007;123(2):1195–1205.

Read RW, Black RM. J Chromatogr A 1999;862(2):169–177. [PubMed: 10596974]

Sacks V, Eshkenazi I, Neufeld T, Dosoretz C, Rishpon J. Anal Chem 2000;72(9):2055–2058. [PubMed: 10815965]

Schulze H, Schmid RD, Bachmann TT. Anal Chem 2004;76(6):1720–1725. [PubMed: 15018574]

Simonian AL, Good TA, Wang SS, Wild JR. Anal Chim Acta 2005;534(1):69–77.

Su XD, Li SFY. Anal Chim Acta 2001;429(1):27–36.

Wessels D, Barr DB, Mendola P. Environ Health Persp 2003;111(16):1939–1946.

Worek F, Koller M, Thiermann H, Szinicz L. Toxicology 2005;214(3):182–189. [PubMed: 16051411]

Yu HZ, Rowe AW, Waugh DM. Anal Chem 2002;74(22):5742–5747. [PubMed: 12463357]

Zhang, XJJHX.; Wang, J. Electrochemical sensors, biosensors and their biomedical applications. Academic Press of Elsevier; San Diego, CA, USA: 2007.

Wang H, Wang J, Timchalk C, Lin YH. Anal Chem 2008;80 (22):8477–8484. [PubMed: 18855408]
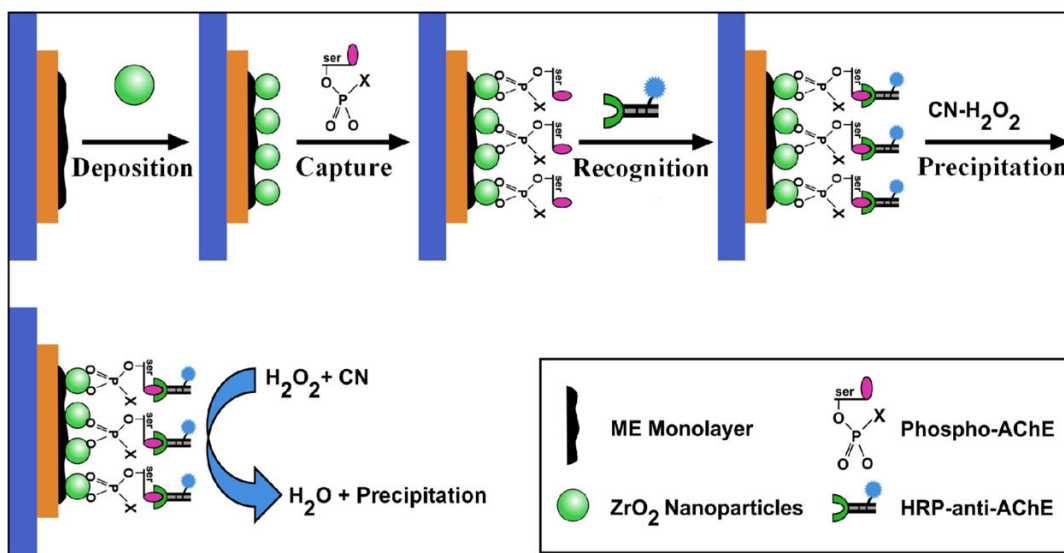
Fig. 1.
Schematic illustration of the principle and process for ZrO_2 adsorption-based EQCM immunoassays for Phospho-AChE, including the ME monolayer modification, ZrO_2 film electro- deposition, Phospho-AChE capture, HRP-anti-AChE recognition, and HRP-catalytic precipitation of insoluble product towards amplified EQCM immunoassays.
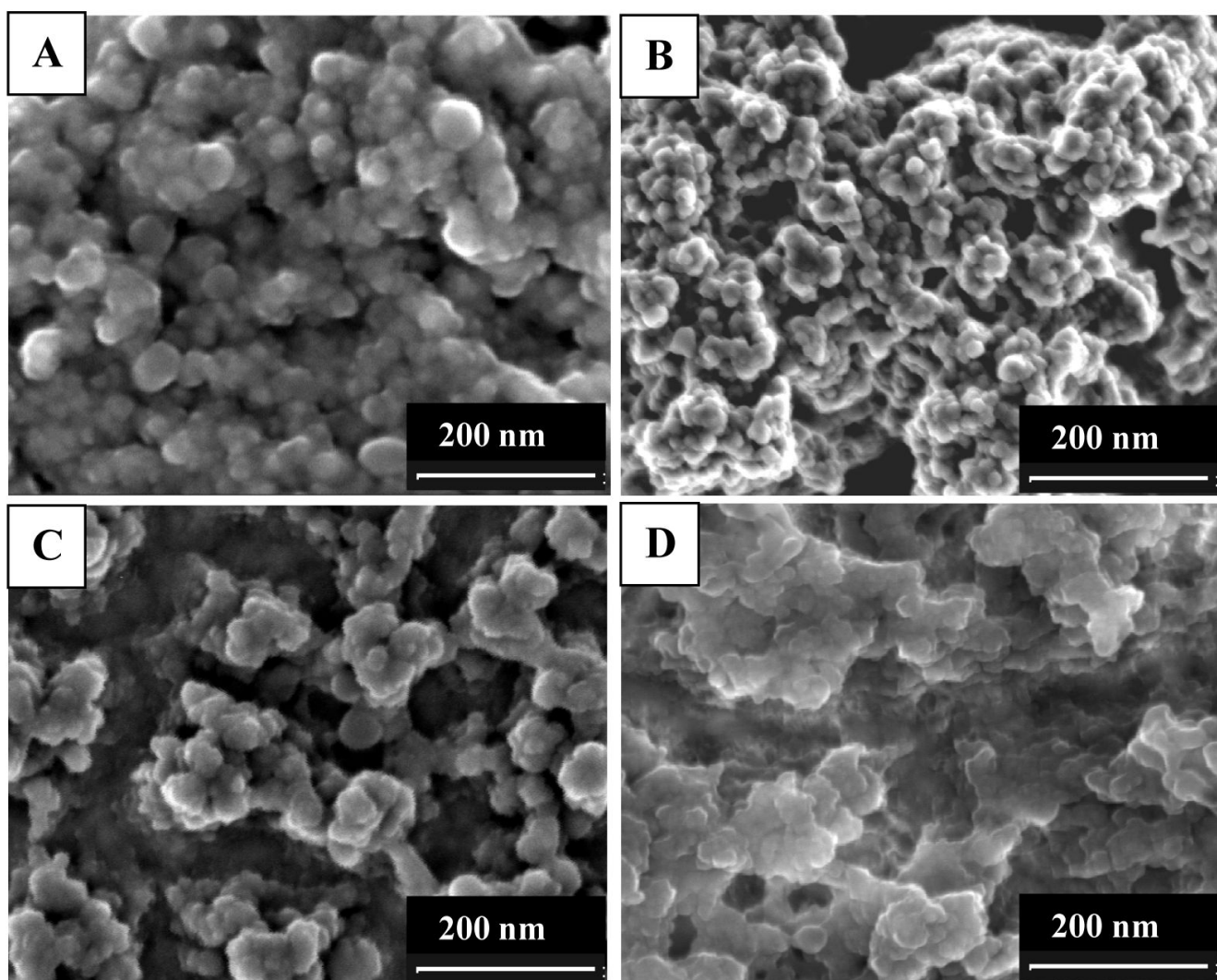
Fig. 2.
SEM images of ZrO_2 film formed on the (A) ME-functionalized and (C) bare gold electrodes of the crystals, corresponding to (B, D) the final H_2O_2-oxidized precipitation of CN substrate by enzyme catalysis in the immunoassays, respectively.
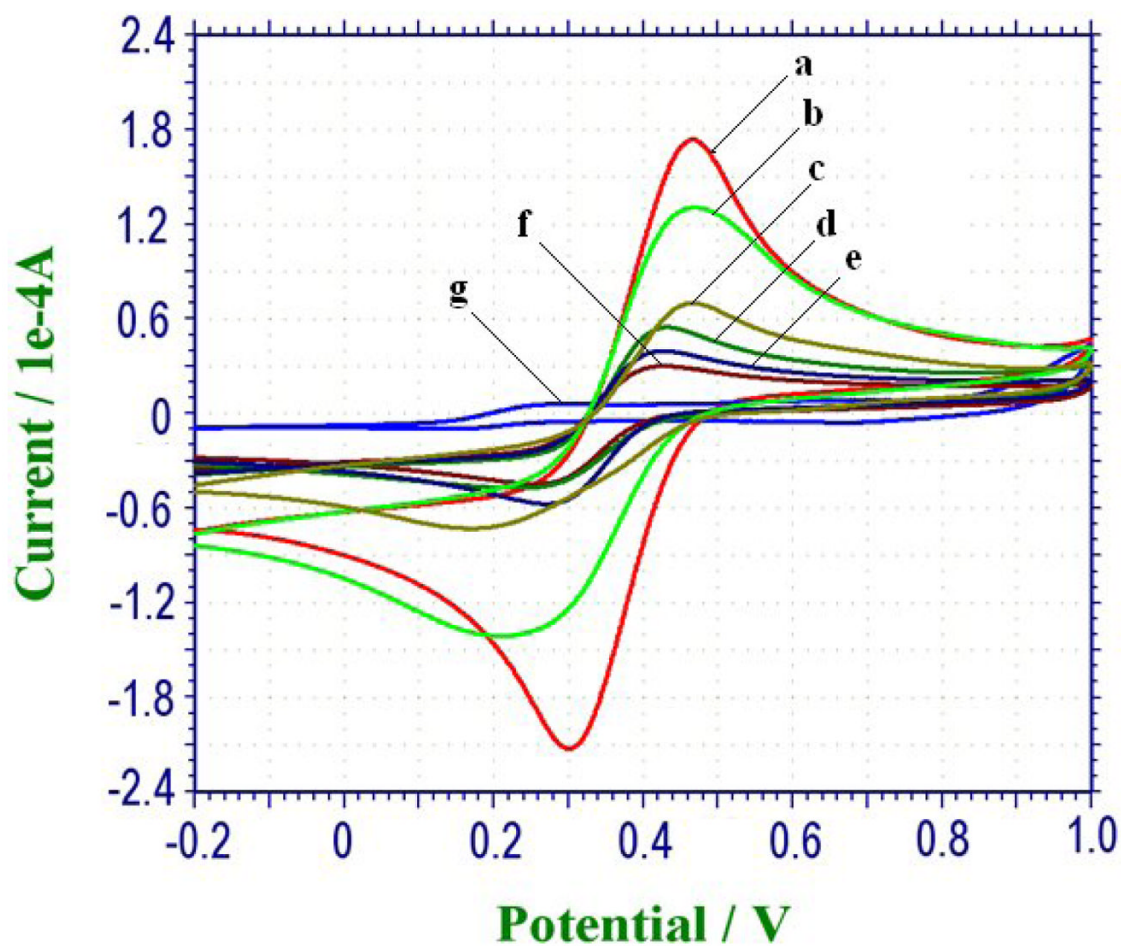
Fig. 3.
Cyclic voltammograms of EQCM characterizing the stepwise buildup process of the sensor in 5 mM $[Fe(CN)_6]^{4-/3-}$ solution (0.01 M, with 0.1 M KCl) at 100 mV s^{-1}, where curve a-g correspond to the crystals modified with: bare, ME monolayer, ZrO_2, Phospho-AChE, BSA-PEG, HRP-anti-AChE, and H_2O_2-oxidized precipitation of CN by enzyme catalysis.
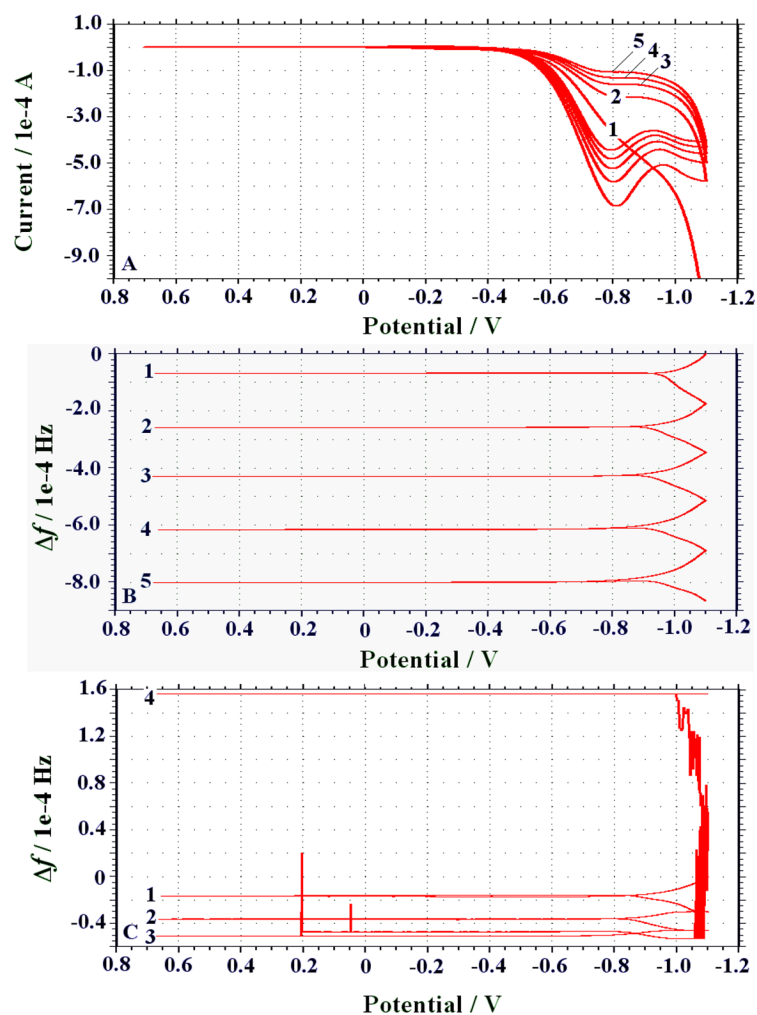
Fig. 4.
Real-time EQCM monitoring of ZrO_2 film electrodeposited onto the ME-modified crystal shown by (A) electrochemical CVs and (B) Δf, comparing with (C) Δf for ZrO_2 electro-deposited on bare gold electrode at a scan rate of 20 mV s^{-1}.
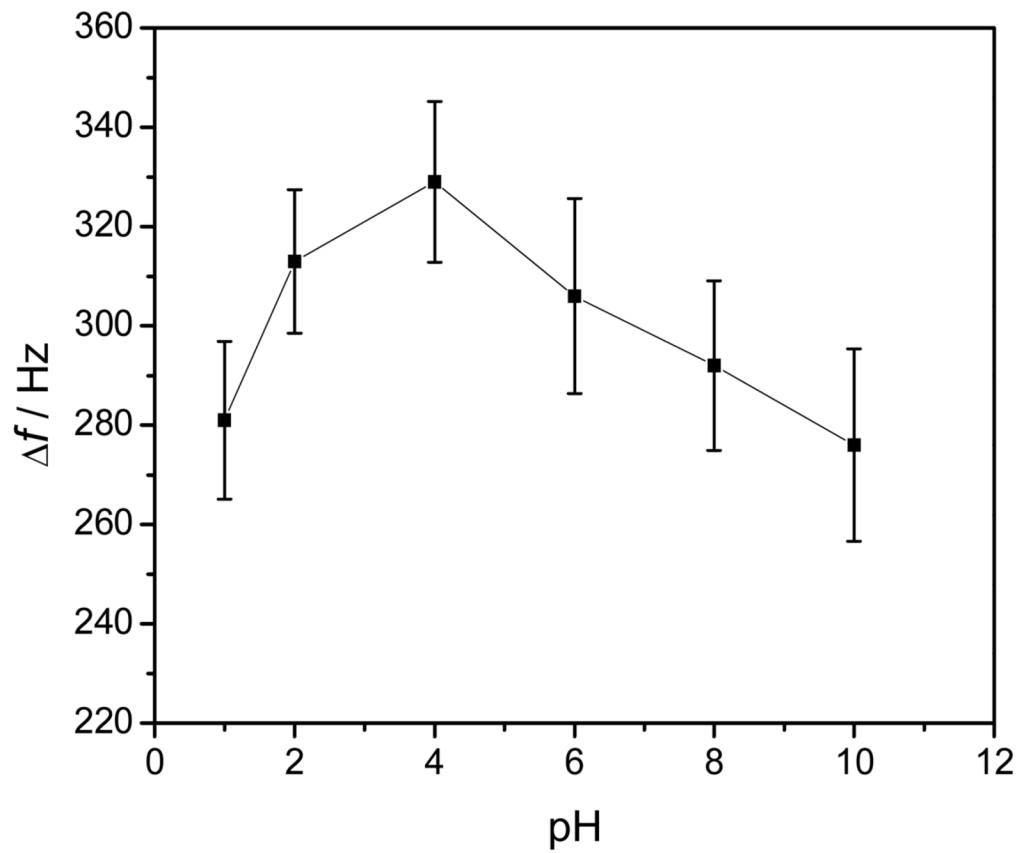
Fig. 5.
The pH dependent adsorption of Phospho-AChE onto ZrO_2 film electrodeposited on the ME-modified crystal. The detections of 0.1 nM Phospho-AChE were performed in the acetate or PBS buffer solutions with different pH values.
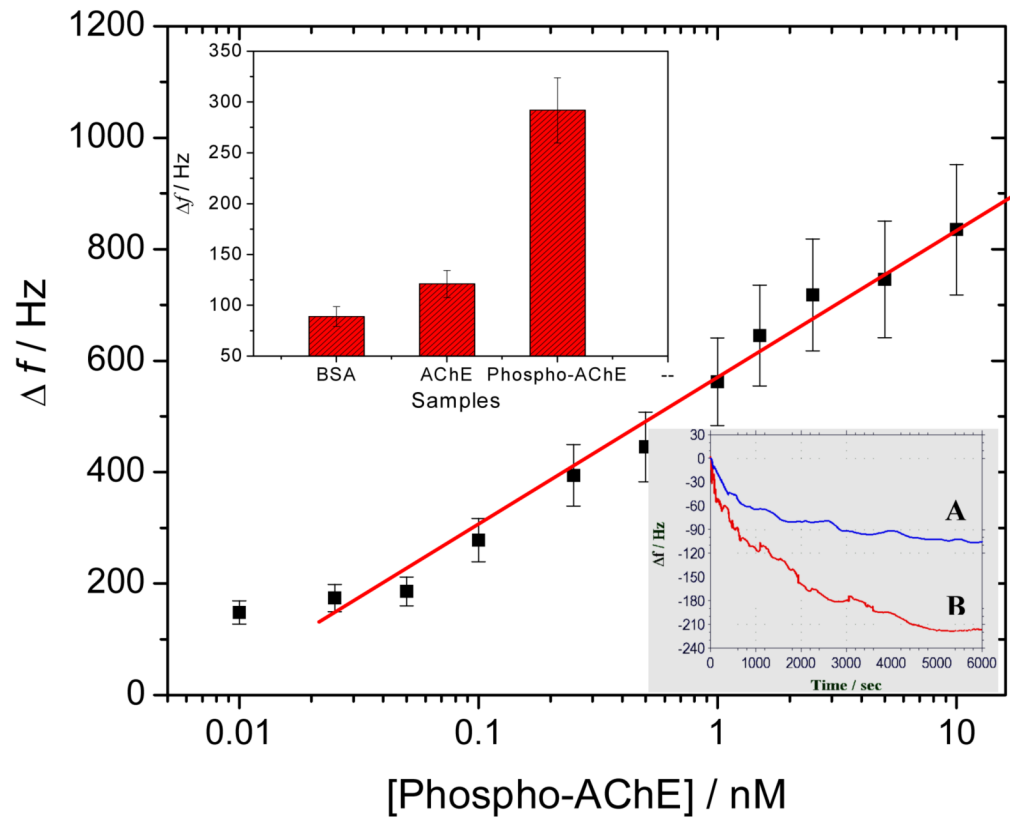
Fig. 6.
Calibration curve plotted on a semi-log scale for detecting Phospho-AChE in plasma samples, with a detection limit of 0.020 nM. The top insert shows the comparison of final Δf responses of immunoassays for BSA (10 mg ml^{-1}), AChE (0.1 nM) and Phospho-AChE (0.1 nM), and the bottom insert manifests the real-time EQCM monitoring for the direct adsorptions of 0.5 nM (A) AChE and (B) Phospho-AChE onto the ZrO$_2$-coated crystals.